WORLD METEOROLOGICAL ORGANIZATION

GLOBAL ATMOSPHERE WATCH

No. 4 – SEPTEMBER 2026

WMO OZONE AND UV BULLETIN

State of the ozone layer in 2025

Wolfgang Steinbrecht, Antje Inness, Mark Weber

About 90% of atmospheric ozone resides in the stratosphere. If all this ozone were brought down to the Earth's surface, the resulting layer of pure ozone would be only approximately 3 millimetres thick. Yet, this thin layer blocks nearly all dangerous short-wave ultraviolet (UV) radiation from the Sun and protects life on Earth. The thickness of the ozone layer, known as total column ozone, is traditionally expressed in Dobson Units (DU). One DU corresponds to 0.01 millimetres of total column ozone, so 3 millimetres corresponds to 300 DU.

Ozone varies geographically and over time as a result of a balance between continual production and destruction by chemical processes, as well as atmospheric transport. Chemical ozone loss due to anthropogenic ozone-depleting substances plays an important role in long-term ozone changes on decadal timescales (*Scientific Assessment of Ozone Depletion: 2022*) and in the formation of springtime polar "ozone holes". This severe springtime ozone depletion requires the right meteorological conditions, which occur almost every austral winter above Antarctica but only every 5 to 10 years in the northern hemisphere (NH). Global inter-annual ozone variations are driven to a large degree by meteorological transport conditions (Chipperfield et al., 2018): at mid- and high latitudes by planetary wave activity and stratospheric warmings; in the tropics and subtropics by residual circulations associated with the equatorial Quasi-Biennial Oscillation (QBO) (Baldwin et al., 2001) or with El Niño/La Niña (Benito-Barca et al., 2022). Figure 1 shows the difference in annual mean total column ozone compared with the climatological long-term distribution (obtained over the period 2003–2022) for each of the last four years. In 2024 and 2025, total column ozone was above average (positive anomalies) over large parts of the southern hemisphere (SH). Both years had relatively active planetary wave driving in the SH, resulting in enhanced poleward ozone transport and small Antarctic ozone holes (see below in this Bulletin).

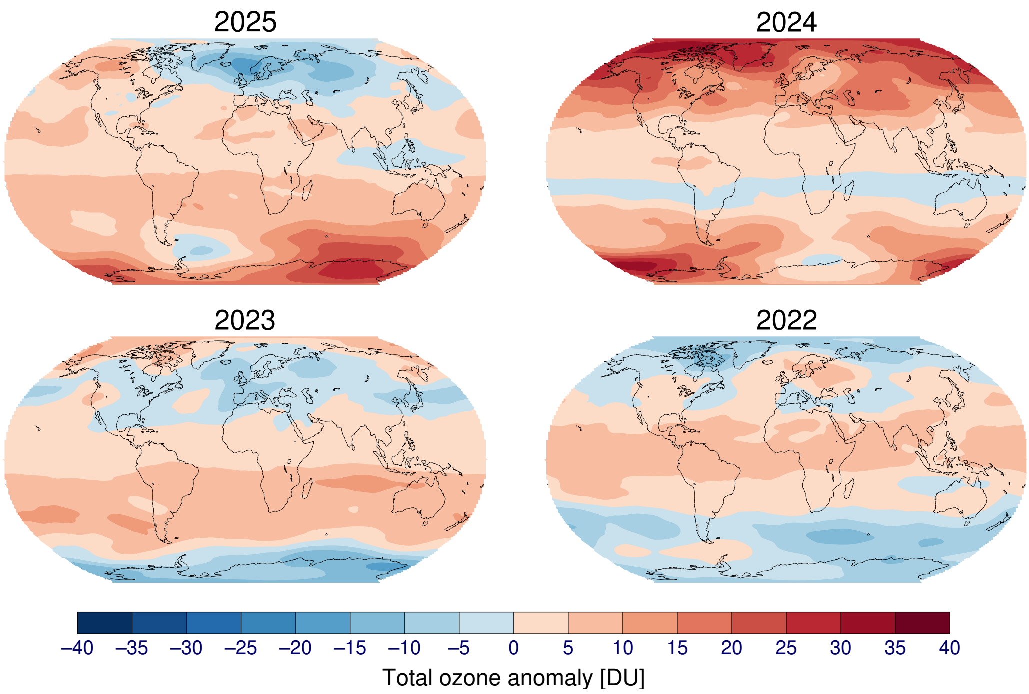

Figure 1. Deviation of recent annual mean total column ozone from its geographic long-term average distribution. Deviations, also called anomalies, are measured in DU. A 30 DU anomaly corresponds to an approximately 10% change in total column ozone.

Source: This map was provided by Antje Inness in July 2026 and may not fully align with United Nations and WMO map guidance. It is based on results from the Copernicus Atmospheric Monitoring Service Reanalysis (Inness et al., 2019).

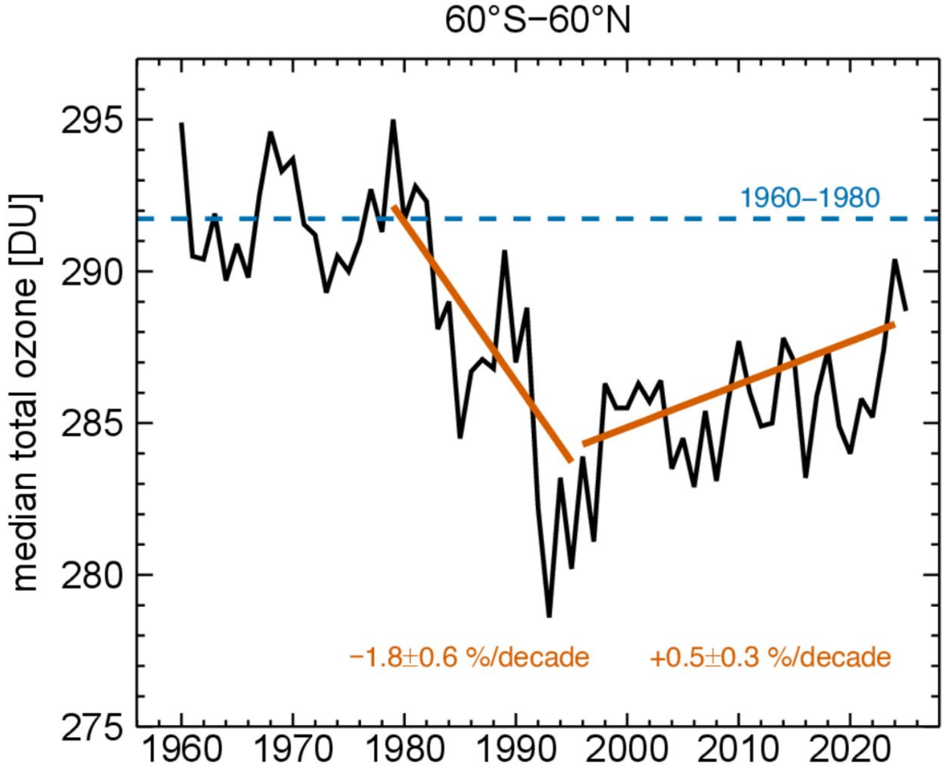

Figure 2. Long-term evolution of annual mean total column ozone, averaged from 60°S to 60°N. The median of available satellite and ground-based datasets is shown. The trend lines were obtained using a multilinear regression model that accounts for key sources of inter-annual variability. The uncertainty is 2σ (95% confidence interval). The ODS-related ozone decline from the 1960s to the 1990s can be clearly seen, as can the beginning of the recovery of ozone starting in 2000.

Source: Adapted from Weber et al. (2022)

In comparison, in 2022 and 2023 there were negative ozone anomalies over large parts of the SH due to reduced poleward transport and chemical ozone reduction after the exceptional Hunga Tonga volcanic eruption in February 2022, as well as above-average ozone-hole sizes (see past Bulletins).

In the NH, total column ozone in 2025 was below average (negative anomalies) in a large region extending from Greenland and Europe to Central Asia, northern Japan and the Kamchatka Peninsula. These negative NH anomalies were due to weak poleward transport and a strong Arctic winter vortex in January and February 2025, causing significant chemical ozone depletion and very low total column ozone in February and March over Eurasia. In contrast, total column ozone in 2024 was well above normal over NH mid- and high latitudes due to strong poleward ozone transport and the very early breakup of a weak polar vortex.

The large year-to-year variability in ozone makes the long-term decline since the 1960s until the early twenty-first century difficult to see in Figure 1. Analyses of longer-term observations show that this decline has been stopped thanks to the successful banning of ozone-depleting substances (ODSs) by the Montreal Protocol and its amendments. ODS concentrations in the atmosphere are now declining slowly. Figure 2 indicates that since 2000, the ozone layer has been recovering, with superimposed year-to-year variations. Full recovery is, however, not expected for another several decades (*Scientific Assessment of Ozone Depletion: 2022*).

State of the Antarctic ozone hole in 2025

Jos de Laat

The depth and overall extent of the 2025 Antarctic ozone hole were significantly smaller than the 1990–2010 average. The 2025 ozone depletion cycle was one of the least severe in over two decades, with the 2025 ozone hole ranking as the fourth to fifth weakest since severe depletion patterns were observed in 1992 (Newman et al., 2026). The maximum ozone mass deficit (OMD) was 36.7 million tons on 29 September (Figure 3), more than 25% less than the 1990–2010 mean of 50.1 million tons.

The daily development of the 2025 ozone hole began normally in mid-July. A relatively early onset of ozone depletion was observed in late August, while peak ozone depletion rates were observed at the start of September, much earlier in the season than in previous years. In fact, OMD values in October – when peaks are usually observed – were well below the 1990–2010 historical envelope. Shortly after this maximum, a series of planetary-scale wave events in mid-September triggered rapid temperature increases throughout the Antarctic lower stratosphere. These warming events effectively slowed stratospheric ozone depletion for the rest of the season. This smaller-than-average spring depletion in 2025 – as well as in 2024 – marks a clear break from the exceptionally deep and long-lasting ozone holes recorded between 2020 and 2023.

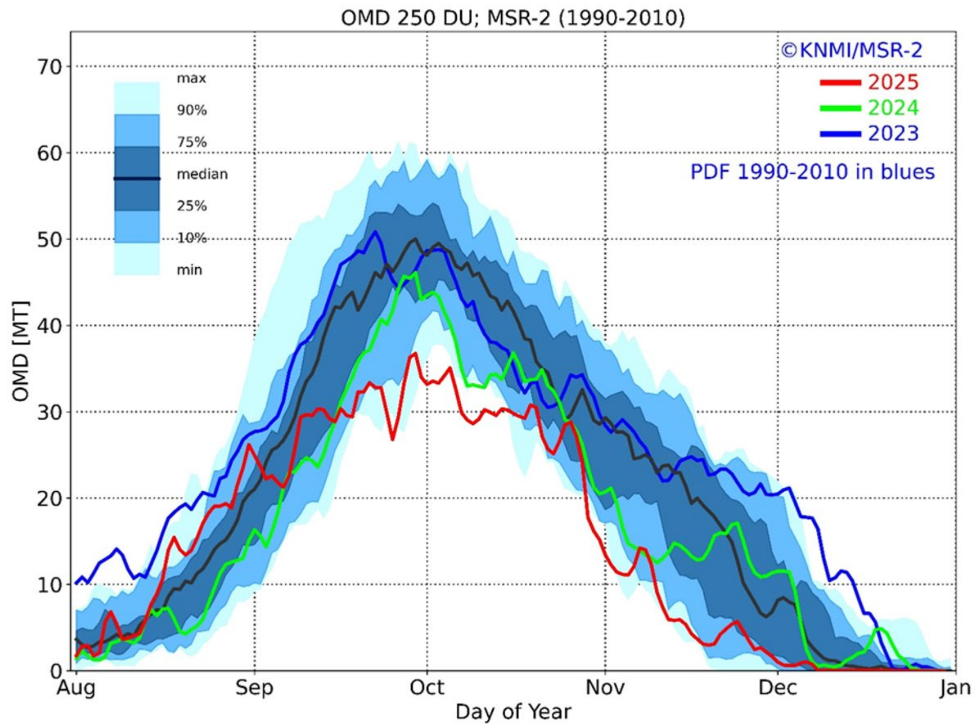

Figure 3. Daily Antarctic ozone mass deficit (OMD) in megatons (MT) relative to the 250 Dobson unit (DU) total ozone column (TOC) level (Strahan et al., 2019) based on multi-sensor reanalysis, version 2 (MSR-2) total ozone reanalysis data (van der A et al., 2015). The OMD is the mass of ozone that would need to be added to bring the TOC within the ozone hole up to the 250 DU level. The red, green and blue lines show the years 2025, 2024 and 2023, respectively. The blue envelope represents the historical envelope and probability distribution of daily OMD data for the period 1990–2010 (PDF = probability density function).

Source: Modified from https://temis.nl/protocols/o3hole/index.php, Royal Netherlands Meteorological Institute (KNMI)

In late October, the Antarctic stratospheric vortex rapidly dissipated, and low total ozone columns largely vanished as air with higher ozone concentrations from outside the vortex was mixed in, although vortex remnants around Antarctica remained detectable in total ozone until early December. Nevertheless, the early disintegration of the vortex further distinguished 2025 from the exceptionally long-lasting ozone holes recorded at the start of the decade. 2024 and 2025 support various analyses indicating that the causes of those anomalous years need to be sought in natural variability. Additionally, the observations from 2024 and 2025 align with the expected long-term decline in stratospheric ozone depletion due to gradually decreasing atmospheric levels of ozone-depleting substances.

100 years of ozone measurements in Switzerland: Celebrating the world's longest continuous ozone time series

Eliane Maillard Barras and Julian Gröbner

The year 2026 marks 100 years of continuous total ozone measurements at Arosa/Davos, Switzerland, the world's longest uninterrupted ground-based total ozone record. Over the past century, this dataset has been central to key scientific discoveries, from the Umkehr effect – the atmospheric optical phenomenon that provided the first observations of the approximate height of the ozone layer – to establishing the pre-chlorofluorocarbon (CFC) ozone baseline and tracking the decrease of ozone in the 1980s and the subsequent stabilization and recovery of the ozone layer.

To celebrate this milestone, MeteoSwiss and the Physikalisch-Meteorologisches Observatorium Davos World Radiation Center (PMOD/WRC) hosted a scientific symposium on 25 July 2026 at the observatory in Davos. The event concluded with a public talk retracing the history of the Arosa/Davos ozone time series, from the first measurements by F. W. Paul Götz on 23 July 1926 in Arosa to the transfer of the automated Dobson spectrophotometer triad to Davos in 2021.

Compared to the 1964–1980 average, present-day total ozone is 2% lower for the northern hemisphere mid-latitudes (35°N–60°N). While ozone recovery has been observed in the upper stratosphere, total column ozone has not shown a significant recovery trend in this region so far, most likely due to confounding changes in the upper and lower stratosphere and the troposphere.

From 2011 to 2021, over a nearly 11-year period, ozone-measuring instruments were progressively transferred from Arosa to Davos to provide an extended period of simultaneous measurements at both locations in order to ensure the continuity of the combined dataset. The subsequent analysis showed that the relocation of the ozone measurements from Arosa to Davos resulted in a difference of approximately 0.3% of total column ozone, which is representative of the differential column of ozone contained in the height difference of 260 m between Arosa and Davos.

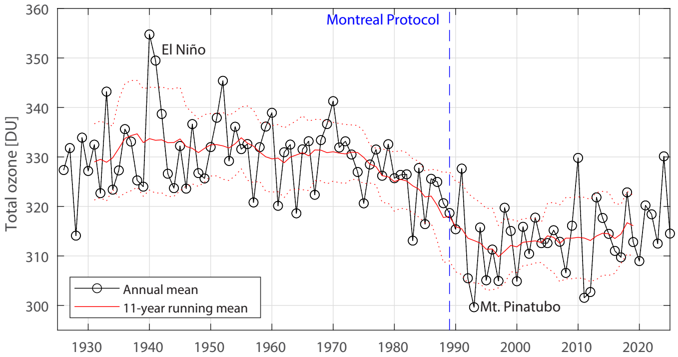

Figure 4. The world's longest ground-based total column ozone observation time series: Arosa/Davos, 23 July 1926–present
Source: Rolf Rüfenacht, MeteoSwiss

The century-long Arosa/Davos record shown in Figure 4 provides a unique dataset for evaluating models and demonstrates that ground-based observations can and should be used to improve estimates of ozone return dates. Although the trend in total ozone became positive a few years after the Montreal Protocol was signed, the total column ozone signal shows high inter-annual variability. This variability is mostly driven by atmospheric dynamics and transport, but also, as indicated in the figure, by extraordinary events such as the 1991 eruption of Mount Pinatubo in the Philippines, which dispersed material, including chlorine-containing substances, high into the stratosphere. In 2011, the lows observed in the Davos record were instead closely linked to the stability of the Arctic vortex, which led to more ozone depletion.

These observations have played a key role in understanding the evolution of total ozone in the atmosphere over the last century. Their value reinforces the importance of continued global ozone monitoring, particularly in detecting the next stages of ozone recovery, understanding the impacts of climate change and providing a basis for guiding policy.

Sustaining the global ozone observing network

Irina Petropavlovskikh, Matt Tully, Sergio Moreno

The 1985 Vienna Convention and the 1987 Montreal Protocol successfully phased out ozone-depleting substances globally, initiating a gradual multi-decadal recovery of the ozone layer. The WMO Global Atmosphere Watch (GAW) network has long provided the critical, high-quality ground-based total column ozone observations required to accurately monitor ozone and ensure that long-term changes can be understood. Traditionally relying primarily on highly stable Dobson and Brewer spectrophotometers, the network fulfils Global Climate Observing System (GCOS) standards for long-term monitoring. Over recent decades, the number of active Dobson and Brewer stations has gradually decreased from around 130 in the early 2000s to 110 today, while the number of filter instruments has approximately halved. In contrast, the number of next-generation array spectrometers, such as Pandora instruments, has grown rapidly over the last few years. However, these instruments have been deployed with a focus on measurements relevant to air quality, and their suitability for long-term stratospheric ozone monitoring is still being established. One of the challenges facing the WMO networks is the need for regular instrument calibration. Many regional calibration centres lack the capacity to host instruments from their regions, train operators and fund intercomparison campaigns. These campaigns are costly to conduct and require extensive support from WMO, but they are important for building capacity and camaraderie in regional communities and for ensuring the traceability of the global network.

A recent joint event successfully combined three activities to maximize scientific, technical and capacity-building benefits: the 20th Regional Brewer Calibration Centre for Europe (RBCC-E) Calibration and Intercomparison Campaign, the 6th African Dobson/Brewer Intercomparison, and a WMO-certified Operators Course. The joint event was hosted by the Spanish National Institute for Aerospace Technology (INTA) and funded by the General Trust Fund for Financing Activities on Research and Systematic Observations Relevant to the Vienna Convention (GTF), with support from WMO/GAW, the Spanish State Meteorological Agency (AEMET), the German Weather Service (DWD), the South African Weather Service (SAWS) and INTA. The event successfully brought together more than 50 specialists from 16 countries and involved 10 Dobson spectrophotometers, 20 Brewer spectrophotometers and 6 BiTec Sensor (BTS) spectrometers. Conducting these side-by-side campaigns allowed experts to better evaluate how instruments such as BTS spectrometers, which use newer technologies, can support and integrate into existing Dobson and Brewer networks.

The campaign demonstrated a generally high level of performance across the Brewer network, with approximately half of the participating instruments showing ozone deviations below 1% relative to the reference Brewer. African participation was particularly significant, with instruments from Algeria, Egypt, Kenya, Uganda and South Africa being calibrated and their operators receiving technical support and training.

The campaign highlighted the value of combining Dobson, Brewer, BTS and future instrument intercomparisons within a single event, fostering collaboration across monitoring communities and improving the consistency of global ozone observations used for climate studies, satellite validation and assessment of ozone-layer recovery. Follow-up activities will include distributing calibration reports, providing technical support, reviewing standard operating procedures and providing data-submission assistance to ensure sustained improvements in observational quality and network performance.

Another important intercomparison campaign took place in Tsukuba, Japan in March 2026. The seventh WMO/GAW Regional Intercomparison of Dobson Spectrophotometers for Asia brought together instruments from India, Pakistan and Thailand and the regional standard maintained by the Regional Dobson Calibration Centre for Asia (RDCC-A).

Experts from DWD (which hosts the Regional Dobson Calibration Centre–Europe) and the United States of America National Oceanic and Atmospheric Administration (NOAA) (which hosts the World Dobson Calibration Centre) provided technical advice to the participants. The campaign marked a bittersweet milestone as the Japan Meteorological Agency (JMA) announced the closure of two Dobson calibration hubs which provided crucial support to the WMO GAW Programme: the Quality Assurance/Scientific Activity Centre on Total Ozone (Dobson instruments) for Asia and the South-West Pacific (QA/SAC-TO), after 31 years, and the Regional Dobson Calibration Centre for Asia (RDCC-A), after 24 years. These closures have created a critical gap and have increased the urgency for the Dobson network to secure a new host country or institution – this is vital in order to ensure that the calibration campaigns can continue and that the RDCC-A can remain operational.

To ensure the continuity and global coverage of ground-based ozone monitoring during a period of technological transition and resource constraints, WMO GAW has led the development of a strategy paper, with the participation of a wide variety of relevant experts representing different networks and interests. This paper, submitted to the Bulletin of the American Meteorological Society, makes a number of important recommendations. New emerging instruments such as BTS and Pandora need to be extensively tested and compared to the current reference instruments in a wide variety of conditions, and algorithms and procedures need to be developed for common use. At the same time, national agencies are urged to continue operating existing Dobson and Brewer programmes and calibration centres for as long as possible and to support the relocation of surplus instruments to priority locations. WMO GAW will continue to play a crucial role in facilitating the many actions required to achieve a sustainable global ozone network over the coming decade.

Cloud-modified local UV forecasts from the RIVM/KNMI UV indexer

Jos de Laat , with input from Arjan van Dijk, Jos van Geffen and Michiel van Weele

WMO coordinates global surface ultraviolet (UV) radiation monitoring to safeguard public health. While traditional weather reports provide broad regional to national indicators of solar intensity, localized cloud cover creates rapid, significant variations on the ground. To bridge this operational gap and deliver real-time analytics of locally available ambient UV radiation, the National Institute for Public Health and the Environment (RIVM), alongside the Royal Netherlands Meteorological Institute (KNMI), has developed the "Zonkrachtwijzer" (UV indexer).

Traditional UV alerts rely on the classical UV index, which represents the daily maximum level of radiation based on ozone thickness, solar zenith angle and cloud-free conditions. However, UV exposure is strongly modified by moving clouds. The UV indexer, developed jointly by RIVM and KNMI, aims to overcome this limitation by adjusting the classical clear-sky index using real-time geostationary satellite cloud observations, allowing users to obtain realistic, time-varying information graphically via an interactive map. The current domain only covers the European territory of the Kingdom of the Netherlands, but the underlying data could, in principle, be produced worldwide. Users interact with the platform in two main ways: either by entering a specific street address or postal code to geolocate the address or by clicking directly on a high-resolution map to drop a pin.

Once a location is selected, the application processes a multi-layered data stream to generate a customized solar safety profile featuring three core components, shown in Figure 5. First, a dual-line temporal tracking graph plots the maximum expected UV curve as a solid line to show theoretical clear-sky intensity, alongside the measured UV curve as a line with dots, which displays the actual, cloud-corrected UV index and is updated continuously. Second, an operational risk scale and colour legend dashboard translates numbers into health metrics, where green (UV index 1–2) means virtually no risk or negligible risk; yellow (UV index 3–4) indicates moderate or emerging risk requiring protection; orange (UV index 5–6) signifies strong or high risk of rapid sunburn requiring active protection and red (UV index 7+) represents very strong or extreme risk to skin and eyes. This Dutch colour coding intentionally deviates from WMO guidelines because the Kingdom of the Netherlands rarely experiences a UV index of 8, so the red threshold was lowered to 7 to make the public better aware of the severity of the risk. Third, an automated behavioural protection advice system triggers concrete safety instructions, including exposure limits for infants and toddlers under two, recommendations for protective clothing, hats and UV sunglasses, reapplication schedules for broad-spectrum SPF 30+ sunscreens and advice to seek shade during the peak hours of 12:00 to 15:00.

To generate hyper-local output, the application fuses multi-layered data onto a 0.05° by 0.05° spatial resolution grid, refreshing every 15 minutes with cloud cover data from geostationary satellites. Processing these multi-spectral observations requires substantial computational steps, resulting in an average delay of 30 to 45 minutes between actual measurement by the satellite and publication of the resulting map on the website. Quietly launched in early summer 2025, the application was rapidly adopted, and feedback analysis showed that users highly valued it, giving it an average rating of 8.9 out of 10.

Formally in a pilot stage, several next steps are planned for further development and outlook. Developers are currently evaluating data against RIVM and KNMI ground-based UV measurement equipment for validation. The Belgian Royal Meteorological Institute (KMI) is preparing to extend map coverage into neighbouring Belgium, for which KNMI has made data operationally available. Furthermore, new satellite measurements of cloudiness at 10-minute intervals and finer spatial resolution are planned to replace current satellite data with a possibly further refinement to 2.5-minute intervals. Finally, future predictive mapping efforts will include further collaborations with other European weather services for seamless cloud pattern observation–prediction to eliminate latency and even provide UV predictions one to two hours in advance.

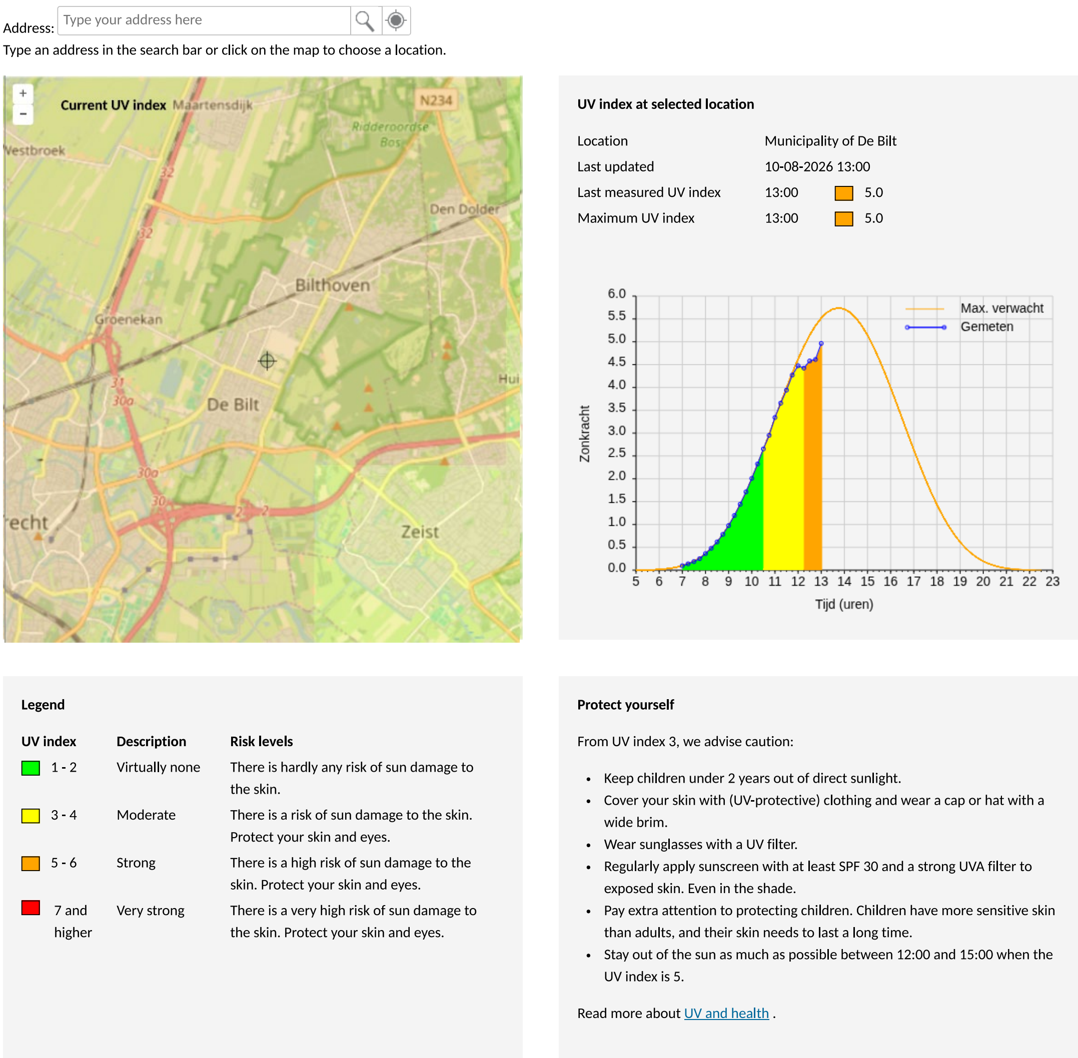

Figure 5. Screenshot of the UV indexer (*Zonkrachtwijzer* in Dutch) on the RIVM website. Entering an address or clicking on a map displays a graph showing the maximum expected UV index (solid line) and the measured UV index (dotted line) throughout the day for that address. The box at the bottom left shows the colour legend for the different risk levels, while general advice regarding the UV index is provided at the bottom right.
Source: RIVM

UV monitoring in the twenty-first century – why we need it and how we can implement it on a large scale

Cornelia Baldermann, Sebastian Lorenz, Daniela Weiskopf, Markus Laufmann, Raul R. Cordero, Julian Gröbner

The monitoring of surface UV radiation became a focus of scientific research as early as the mid-1980s due to changes in the ozone layer and the associated potential increase in ground-level UV radiation and corresponding negative effects on human health.

While substantial progress has been made in addressing ozone depletion, the societal relevance of monitoring UV radiation remains high. An increase in surface UV radiation affects public health and terrestrial and aquatic ecosystems and accelerates the degradation of materials. UV radiation drives the fragmentation, aging and chemical transformation of plastics into microplastics and nanoplastics. The strength and duration of UV exposure largely determine how quickly plastics degrade, how toxic they become and how they interact with the environment (see, for example, Andrady et al., 2023). Changes in UV exposure serve as a sensitive indicator of broader atmospheric change.

In numerous regions, measurements over the past decades show a significant increase in the annual UV dose, an increase in the number of days with high UV index values and more frequent elevated UV index values, particularly in the spring and early summer (Chatzopoulou et al., 2024; Lorenz et al., 2024). Since the mid-1990s, UV radiation has increased significantly across Europe. At some UV monitoring stations, annual UV doses have risen by as much as 20% since 1995, exceeding the changes associated with the decline in total ozone column (TOC) between 1975 and 1990. Ground-based measurements show that this increase has been driven primarily by a reduction in cloud cover, resulting in an increase in annual sunshine duration. It is also attributable, in part, to changes (reductions) in aerosol concentrations (Fountoulakis et al., 2016) through the direct aerosol effect (ADE). In Europe, the increase in surface solar radiation is attributable to the influence of clouds (80%) and ADE-related changes (20%) (Segado-Moreno et al., 2026). An increase in surface UV on cloudless days leads to higher UV exposure. An increase in cloud-free days would therefore lead to more days with a

Figure 6. Self-contained broadband radiometer with solar panel
Credit: Markus Laufmann; © Federal Office for Radiation Protection (BfS)

high UV index and high UV exposure, which would increase the risk of skin cancer and other UV-related diseases among exposed populations. The global burden of UV-induced skin cancer rose significantly between 1990 and 2021; particularly rapid increases have been observed in regions with a medium sociodemographic index (Zhou et al., 2025).

In light of this trend, targeted and effective UV protection measures are of paramount importance. A key foundation for this is knowledge of current UV intensity, as expressed by the UV index, which was developed by the late Canadian atmospheric scientist Thomas McElroy and his colleagues James B. Kerr and David I. Wardle to track the depletion of the ozone layer and now serves as an international health standard for UV protection (World Health Organization (WHO) et al., 2002). Information about the current UV index helps the public understand the need for UV protection measures, apply them and make them a part of their daily lives. The UV index is provided by models based on satellite data and by ground-based measurements. In regions with frequently changing cloud cover, local measurements of UV radiation often provide more reliable values than modelled or satellite-derived values due to the large footprint and limited temporal coverage of satellites. The same applies to areas with significant topographic variability or highly fluctuating air pollution levels.

Spectroradiometers and broadband filter radiometers are the primary ground-based instruments used to measure UV irradiance and calculate the UV index. Spectroradiometers accurately measure discrete wavelengths of light across the solar spectrum and are essential for scientific applications due to their high precision; however, they are too costly and labour-intensive to be used solely to provide UV index information to the public. Broadband filter radiometers measure UV radiation integrally across a broad spectral range and are more cost-effective and easier to operate. They can be deployed by municipalities, schools or private users. However, implementing them can be a challenge due to the need for complex peripheral equipment (cabling, lightning protection and so forth). Broadband instruments also require careful calibration and maintenance to yield high-quality data.

Recently, broadband filter radiometers have become available as self-contained stations that do not require an external power supply (Figure 6). These stations can be set up freely in unshaded locations to measure the UV index. Power is supplied by solar panels and the measured UV index values are transmitted via radio to display devices. This makes these stations suitable for use in public spaces as well as for educational purposes in cities, rural areas and extremely remote regions.

The self-contained stations are equipped with high-quality broadband radiometers that can be calibrated very accurately. The better the calibration, the more accurate the measurements. With a single calibration factor, a well characterized broadband radiometer can achieve an accuracy of a whole-number UV index value during periods relevant to UV protection. The best results are achieved using a calibration matrix that provides a calibration factor based on the solar elevation and total column ozone values. Such calibrations can be performed by calibration laboratories at the Physikalisch-Meteorologisches Observatorium Davos World Radiation Center (PMOD/WRC).

The homogeneity and traceability of UV measurements on a global scale are supported by quinquennial calibration campaigns organized by the World Calibration Center for UV at PMOD/WRC (Hülsen and Gröbner, 2023). During these campaigns all participating broadband filter radiometers are calibrated with uncertainties as low as 3%.

As with all measuring instruments, these broadband radiometers must be maintained regularly to ensure proper functioning. Maintenance includes, among other things, routine cleaning and plausibility checks of the measured values. These can be done by comparing the measured values with the predicted UV index values on cloudless days with little aerosol pollution and well-known surface reflectivity value.

In addition to stationary measuring devices, there are now devices for tracking personal UV exposure, including UV-tracking wristbands, smartphone apps and external UV sensors. However, studies have shown that many of these tools have low accuracy (Bernhard et al., 2023; Salvadori et al., 2020). Looking ahead, UV monitoring in the twenty-first century should aim to sustain and expand sites in underrepresented regions (for example, the tropics and southern hemisphere mid-latitudes) to improve global coverage by using affordable instrumentation. It should also integrate UV measurements with co-located aerosol and cloud observations to support

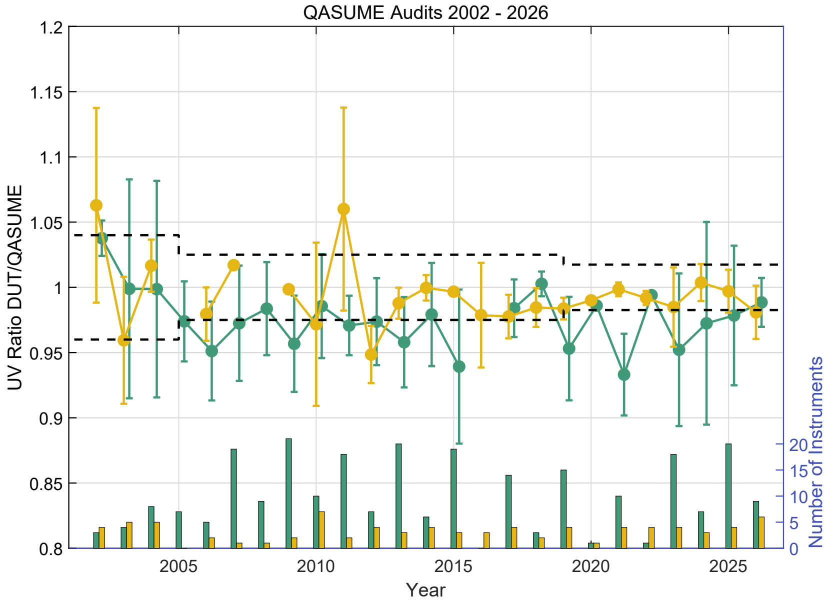

Figure 7. Average yearly ratio of UV site audits to QASUME. The green dots represent comparisons to Brewer spectroradiometers, while the yellow dots represent comparisons to scanning spectroradiometers from other manufacturers. The lower bars represent the number of instrument audits per year. The dashed lines represent the expanded relative uncertainty of QASUME.

Source: Julian Gröbner and Gregor Hülsen, PMOD

climate analyses and the validation of chemistry-climate models (CCMs) and Earth system models (ESMs) and enhance data interoperability with satellite missions and emerging networks (such as PANDORA and SAOZ). In addition, it should invest in capacity-building and calibration infrastructure, especially in the Global South, ensuring long-term traceability and continuity of records, and leverage UV datasets for multidisciplinary research beyond public health, including climate–biosphere interactions and material development under changing radiation and climate regimes. Reliably measured UV index values should be accessible to everyone, anytime and anywhere. Modern, self-contained broadband radiometers now make this possible worldwide.

25-year UV calibration campaigns (QASUME)

Julian Gröbner and Gregor Hülsen

The EU-funded project Quality Assurance of Spectral Ultraviolet Measurements in Europe (QASUME) started in 2002 and was initially operated by the Joint Research Centre of the European Commission (Gröbner et al., 2006). The audit activities of the QASUME portable reference spectroradiometer were transferred to the Physikalisch-Meteorologisches Observatorium Davos World Radiation Center (PMOD/WRC) in 2006, where they became part of the central tasks of the WMO World Calibration Center for UV (WCC-UV) in 2016.

In total, 336 site audits were carried out between 2002 and 2026, and 121 instruments at 39 stations were compared to the QASUME spectroradiometer. Typically, four to five site audits are performed per year, usually at European UV monitoring sites. These audits are important for maintaining the quality of spectral UV measurements over long time periods, especially when multiple visits are conducted at the same sites (Fountoulakis et al., 2020; Lakkala et al., 2013, 2018).

The QASUME spectroradiometer has been the reference instrument for the solar UV measurements performed by the European Brewer network since 2005, participating in all campaigns, which are held alternately at El Arenosillo, Spain, and Arosa/Davos, Switzerland *(Eighteenth Intercomparison Campaign of the Regional Brewer Calibration Centre Europe* (GAW Report No. 302)).

Figure 7 shows a summary of the 336 site audits performed between 2002 and 2026. As can be seen, the majority of Brewer spectroradiometers systematically underestimate solar UV radiation (green curve), resulting partly from uncorrected angular response deviations in the global UV entrance optics. On the other hand, the spectroradiometers from other manufacturers (yellow curve) have improved their solar UV measurements over the years, showing very good agreement with QASUME since about 2013.

The results of these QASUME site audits can be found at the WCC-UV website.

Atmospheric monitoring of controlled substances under the ozone treaties and its relevance to the Kigali Amendment to the Montreal Protocol

Sophia Mylona

The 1985 Vienna Convention for the Protection of the Ozone Layer and its 1987 Montreal Protocol on Substances that Deplete the Ozone Layer constitute the cornerstone of the international regime for protecting the stratospheric ozone layer. While the Convention established the framework for scientific cooperation, including on research and systematic observations of the ozone layer, the Protocol introduced legally binding phase-out schedules for the production and consumption of ozone-depleting substances (ODSs). In 2016, the Kigali Amendment expanded the scope of the Montreal Protocol to include hydrofluorocarbons (HFCs), potent greenhouse gases that do not deplete the ozone layer but are used to replace ODSs, with phase-down schedules that extend to the late 2040s for developing country parties. The implementation of the Montreal Protocol has successfully reduced the global production and consumption of ODSs, contributing to the ongoing recovery of the ozone layer while also delivering substantial climate benefits (see *WMO Ozone and UV Bulletin No. 3*).

As parties implement ODS phase-out and HFC phase-down schedules and continue reporting production and consumption data to the Ozone Secretariat, atmospheric monitoring has become increasingly important for assessing whether reported reductions are reflected in observed declines in the atmospheric concentrations of controlled ODSs and HFCs, as well as in inferred emissions.

Over the past four decades, atmospheric measurements have demonstrated significant reductions in the concentrations of controlled ODSs following the implementation of Protocol control measures. In recent years, atmospheric monitoring has proven essential for detecting unexpected emissions. The identification of increasing global emissions of CFC-11 in 2018 underscored the importance of independent atmospheric observations in supporting compliance efforts and highlighted the role of science in enabling timely policy responses. Subsequent atmospheric observations indicated a return towards expected trends following targeted regulatory and enforcement actions undertaken by national authorities.

More recently, atmospheric measurements have shown that global HFC-23 emissions are significantly higher than those inferred from reported data. Two of the Montreal Protocol's assessment panels, the Scientific Assessment Panel (SAP) and the Technology and Economic Assessment Panel (TEAP), have been providing relevant information to the parties to facilitate their consideration of this issue. In addition, the 2026 quadrennial SAP and TEAP assessments, to be finalized by the end of 2026 alongside the assessment of the Environmental Effects Assessment Panel (EEAP), are expected to provide further analysis of the consistency between atmospheric observations and reported data across all controlled substances.

Recognizing the growing importance of these discrepancies, the parties have placed increasing emphasis on enhancing regional atmospheric monitoring under the ozone treaties. Since the detection in 2018 of unexpected increases in CFC-11 emissions and the subsequent consideration of gaps in regional atmospheric monitoring by ozone research managers under the Vienna Convention, several decisions of the parties have called upon SAP, TEAP, the Ozone Secretariat, the

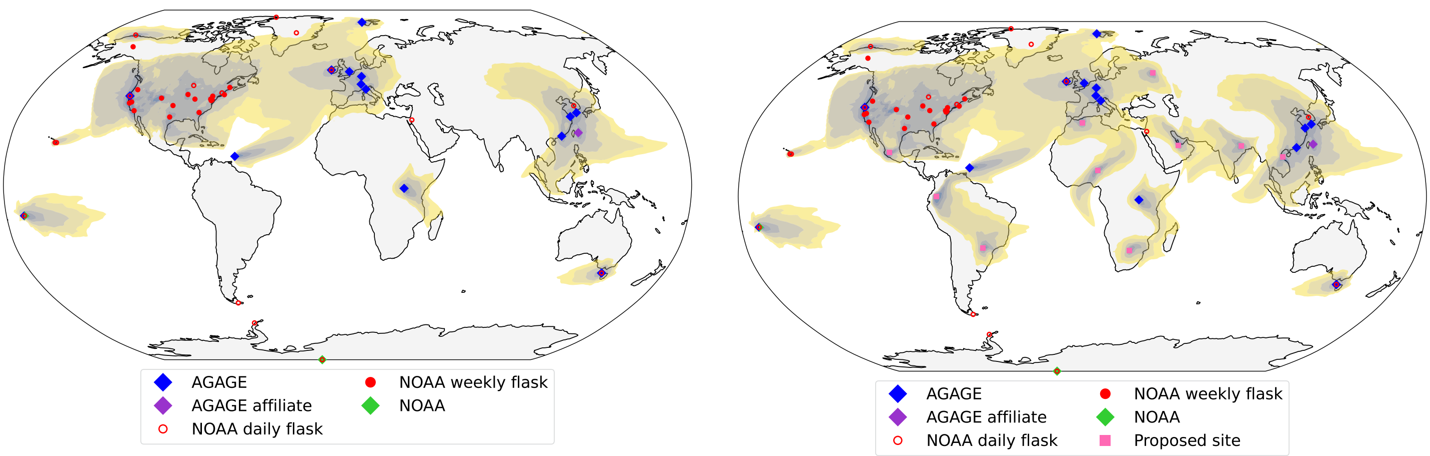

Figure 8: Atmospheric monitoring network coverage under the current and proposed configurations. Left: Existing atmospheric monitoring network coverage. Right: Expected monitoring coverage after establishing stations at the proposed locations. Shaded regions show station sensitivity to annual emissions, indicating areas where regional emissions can be reliably detected and quantified. The blue and purple diamonds denote stations belonging to or affiliated with the Advanced Global Atmospheric Gases Experiment (AGAGE) network. The green diamonds and red circles denote United States of America National Oceanic and Atmospheric Administration (NOAA) sites where flask samples are collected on a daily or weekly basis. The pink squares denote the proposed monitoring station locations to address gaps in regional coverage.

Source: Third-party map. This map was provided by Luke Western, Massachusetts Institute of Technology (MIT), on 6 August 2026 and may not fully align with United Nations and WMO map guidance.

Advisory Committee of the General Trust Fund for Financing Activities on Research and Systematic Observations Relevant to the Vienna Convention and the Executive Committee of the Multilateral Fund for the Implementation of the Montreal Protocol to provide further information and undertake associated activities.

In response, further analyses of the sources, sinks and emissions of controlled substances were conducted; the suitability of potential sites for establishing regional monitoring stations in under-sampled regions around the globe was evaluated (see Figure 8); costs for establishing and operating monitoring stations were estimated, including through the development of a tool to estimate such costs; and funding for supporting pilot projects for such activities was adopted under the Multilateral Fund. Collectively, these efforts reflect the recognition that enhancing regional atmospheric monitoring is essential for complementing national reporting systems and supporting scientific assessments under the ozone regime, thereby helping to verify and sustain the phase-out/reduction schedules achieved under that regime.

As the international community prepares to celebrate the tenth anniversary of the Kigali Amendment on 15 October 2026, ongoing efforts to enhance regional atmospheric monitoring of controlled substances under the Vienna Convention and the Montreal Protocol provide a solid basis for evaluating implementation progress. Together, the complementary frameworks of these treaties strengthen transparency, accountability and evidence-based policymaking, ensuring the continued effectiveness of the ozone regime in protecting the ozone layer and contributing to global climate mitigation.

THE KIGALI AMENDMENT 2016–2026

The Kigali Amendment at ten: A cooling success story

Stephanie Egger Haysmith

Ten years after it was agreed, the Kigali Amendment to the Montreal Protocol stands as one of the most important – and least widely known – global achievements in the fight against climate change. While it rarely makes headlines, the Amendment is already delivering measurable benefits for the climate and offers a powerful example of fruitful international cooperation.

The Kigali Amendment was adopted in 2016 to address the growing use of hydrofluorocarbons, commonly known as HFCs. These chemicals are widely used in everyday cooling technologies such as refrigerators, air conditioners, insulating foams, and some medical and industrial equipment. They were originally introduced as safer alternatives to chemicals that damaged the ozone layer, but scientists later discovered that HFCs are extremely powerful greenhouse gases. Some trap thousands of times more heat than carbon dioxide, even though they remain in the atmosphere for a much shorter time. For example, HFC-134a (a refrigerant used in automobile air conditioning systems) can store over one thousand times more heat per molecule than carbon dioxide.

As extreme heat and record-breaking temperatures become increasingly common, demand for cooling is growing rapidly. Without measures to curb HFC use, these emissions could add substantially to future warming. The Kigali Amendment was designed to prevent that outcome by requiring countries to gradually reduce the amount of HFCs they produce and use.

The Amendment has been ratified by 174 of the 198 Parties to the Montreal Protocol, a treaty that has been described as the most successful environmental agreement in history. Countries follow different timelines depending on their level of development and climate conditions. Developed parties (Article 2) began reducing their HFC use in 2019, while most developing parties (Article 5) are freezing and then gradually cutting their HFC use over the coming decade. Countries with particularly hot climates have been given more time where alternatives are not yet widely available. Despite these differences, all participating countries are working towards the same long-term goal: cutting global HFC use by more than 80% by the late 2040s.

If fully implemented, the Kigali Amendment is expected to prevent up to 0.5 °C of global warming by 2100. The benefits of the Kigali Amendment extend beyond reducing emissions of refrigerant gases. Countries can significantly reduce energy use, cut electricity bills, ease pressure on power grids and increase climate benefits by upgrading equipment while replacing refrigerants.

This makes the Kigali Amendment an incredibly effective tool for climate action. HFCs are short-lived pollutants, and therefore reducing them helps to slow near-term warming while longer-term efforts to cut carbon dioxide continue.

The near-universal acceptance of the Kigali Amendment, including by the world's largest economies, reflects a shared recognition that cooling is essential for health, food security and economic development – but that it must be done in a way that does not worsen the climate crisis. A decade on, the Kigali Amendment is a powerful example of how science-based international cooperation can deliver real results for people and the planet.

References

Andrady, A. L.; Heikkilä, A. M.,;Pandey, K. K. et al. Effects of UV Radiation on Natural and Synthetic Materials. *Photochemical & Photobiological Sciences* **2023**, *22* (5), 1177–1202. https://doi.org/10.1007/s43630-023-00377-6.

Baldwin, M. P. Gray, L. J.; Dunkerton, T. J. et al. The Quasi-Biennial Oscillation, *Reviews of Geophysics* **2001**, *39* (2), 179–229, https://doi.org/10.1029/1999RG000073.

Benito-Barca, S.; Calvo, N.; Abalos, M. Driving Mechanisms for the El Niño–Southern Oscillation Impact on Stratospheric Ozone. *Atmospheric Chemistry and Physics* **2022**, *22* (24), 15729–15745, https://doi.org/10.5194/acp-22-15729-2022.

Bernhard, G. H.; Bais, A. F.; Aucamp, P. J. et al. Stratospheric Ozone, UV Radiation, and Climate Interactions. *Photochemical & Photobiological Sciences* **2023**, *22* (5), 937–989. https://doi.org/10.1007/s43630-023-00371-y.

Chatzopoulou, A.; Tourpali, K.; Bais, A. F. et al. Twenty-first Century Surface UV Radiation Changes Deduced from CMIP6 Models. Part II: Effects on UV Index and Plant Growth Weighted Irradiance. *Photochemical & Photobiological Sciences* **2024**, *24* (1), 113–120. https://doi.org/10.1007/s43630-024-00676-6.

Chipperfield, M. P., Dhomse, S., Hossaini, R., et al. On the Cause of Recent Variations in Lower Stratospheric Ozone. *Geophysical Research Letters* **2018**, *45*, 5718–5726. https://doi.org/10.1029/2018GL078071.

Fountoulakis, I.; Bais, A. F.; Fragkos, K. et al. Short- and Long-term Variability of Spectral Solar UV Irradiance at Thessaloniki, Greece: Effects of Changes in Aerosols, Total Ozone and Clouds. *Atmospheric Chemistry and Physics* **2016**, *16* (4), 2493–2505. https://doi.org/10.5194/acp-16-2493-2016.

Fountoulakis, I.; Diémoz, H.; Siani, A. M., et al. Monitoring of Solar Spectral Ultraviolet Irradiance in Aosta, Italy. *Earth System Science Data* **2020**, *12* (4), 2787–2810. https://doi.org/10.5194/essd-12-2787-2020.

Global Atmosphere Watch (GAW). *Eighteenth Intercomparison Campaign of the Regional Brewer Calibration Centre Europe* (GAW Report No. 302); World Meteorological Organization (WMO): Geneva, 2024.

Gröbner, J.; Blumthaler, M.; Kazadzis, S. et al. Quality Assurance of Spectral Solar UV Measurements: Results from 25 UV Monitoring Sites in Europe, 2002 to 2004. *Metrologia* **2006**, *43* (2). https://doi.org/10.1088/0026-1394/43/2/S14

Hülsen G.; Gröbner, J. *Report of the Third International Solar UV Radiometer Calibration Campaign (UVC-III)* (Global Atmosphere Watch (GAW) Report No. 284); World Meteorological Organization (WMO): Geneva, 2023.

Inness, A.; Ades, M.; Agustí-Panareda, A. et al. The CAMS Reanalysis of Atmospheric Composition. *Atmospheric Chemistry and Physics* **2019**, *19* (6), 3515–3556. https://doi.org/10.5194/acp-19-3515-2019.

Lakkala, K.; Arola, A.; Heikkilä, A. et al. Two Decades of Spectral UV Measurements at Sodankylä. *AIP Conference Proceedings* **2013**, *1531* (1), 883–886. https://doi.org/10.1063/1.4804912.

Lakkala, K.; Arola, A.; Gröbner, J. et al. Performance of the FMI Cosine Error Correction Method for the Brewer Spectral UV Measurements. *Atmospheric Measurement Techniques* **2018**, *11* (9), 5167–5180. https://doi.org/10.5194/amt-11-5167-2018.

Lorenz, S.; Heinzl, F.; Bauer, S. et al. Increasing Solar UV radiation in Dortmund, Germany: Data and Trend Analyses and Comparison to Uccle, Belgium. *Photochemical & Photobiological Sciences* **2024**, *23* (12), 2173–2199. https://doi.org/10.1007/s43630-024-00658-8.

Newman, P. A.; Coy, L.; Cullis, P. et al. 2025 Antarctic Ozone Hole. In State of the Climate in 2025. *Bulletin of the American Meteorological Society* **2026**, *107* (8) [special supplement], S387–S400. https://www.ametsoc.org/ams/publications/journals/bulletin-of-the-american-meteorological-society-bams/state-of-the-climate/.

Salvadori, G.; Leccese, F.; Lista, D. et al. Use of Smartphone Apps to Monitor Human Exposure to Solar Radiation: Comparison between Predicted and Measured UV Index Values. *Environmental Research* **2020**, *183*. https://doi.org/10.1016/j.envres.2020.109274.

Segado-Moreno, L. C.; Ruiz-Arias, J. A.; Montávez, J. P. et al. Past, Current and Future Solar Radiation Trends in Europe: Multi-source Assessment of the Role of Clouds and Aerosols. *Remote Sensing of Environment* **2026**, *333*. https://doi.org/10.1016/j.rse.2025.115122.

Strahan, S. E.; Douglass, A. R.; Damon, M. R. Why Do Antarctic Ozone Recovery Trends Vary? *Journal of Geophysical Research: Atmospheres* **2019**, *124*, 8837–8850. https://doi.org/10.1029/2019JD030996.

van der A, R. J.; Allaart, M. A. F.; Eskes, H. J. Extended and Refined Multi Sensor Reanalysis of Total Ozone for the Period 1970–2012. *Atmospheric Measurement Techniques* **2015**, *8* (7), 3021–3035. https://doi.org/10.5194/amt-8-3021-2015.

Weber, M.; Arosio, C.; Coldewey-Egbers, M. et al. Global Total Ozone Recovery Trends Attributed to Ozone-depleting Substance (ODS) Changes, Derived from Five Merged Ozone Datasets. *Atmospheric Chemistry and Physics* **2022**, *22* (10), 6843–6859. https://doi.org/10.5194/acp-22-6843-2022.

World Health Organization (WHO); World Meteorological Organization (WMO); United Nations Environment Programme (UNEP); International Commission on Non-Ionizing Radiation Protection (ICNIRP). *Global Solar UV Index: A Practical Guide*; WHO: Geneva, 2002.

World Meteorological Organization (WMO). *Scientific Assessment of Ozone Depletion: 2022*. (Global Atmosphere Watch (GAW) Report No. 278). Geneva, 2022.

Zhou, L.; Zhong, Y.; Han, L. et al. Global, Regional, and National Trends in the Burden of Melanoma and Non-melanoma Skin Cancer: Insights from the Global Burden of Disease Study 1990–2021. *Scientific Reports* **2025**, *15* (1). https://doi.org/10.1038/s41598-025-90485-3.

Authors and contributors (in alphabetical order)

Cornelia Baldermann (Federal Office for Radiation Protection (BfS), Germany)
Raul R. Cordero (Universidad de Santiago de Chile, Chile)
Jos de Laat (Royal Netherlands Meteorological Institute (KNMI), Kingdom of the Netherlands)
Stephanie Egger Haysmith (United Nations Environment Programme (UNEP))
Julian Gröbner (Physikalisch-Meteorologisches Observatorium Davos World Radiation Center (PMOD/WRC), Switzerland)
Gregor Hülsen (PMOD/WRC, Switzerland)
Antje Inness (European Centre for Medium-Range Weather Forecasts (ECMWF))
Markus Laufmann (BfS, Germany)
Sebastian Lorenz (BfS, Germany)
Eliane Maillard Barras (MeteoSwiss, Switzerland)
Sergio Moreno Valero (WMO)
Sophia Mylona (UNEP)
Irina Petropavlovskikh (Cooperative Institute for Research and Environmental Science (CIRES), University of Colorado, Boulder, United States of America)
Wolfgang Steinbrecht (Deutscher Wetterdienst (DWD), Germany)
Matt Tully (Bureau of Meteorology (BOM), Australia)
Mark Weber (University of Bremen, Germany)
Daniela Weiskopf (BfS, Germany)
Luke Western (Massachusetts Institute of Technology (MIT), USA)

Editorial team (in alphabetical order)

Leilani Dulguerov (WMO)
Gordon Labow (National Aeronautics and Space Administration (NASA) Goddard Space Flight Center (GSFC), USA)
Paolo Laj (WMO)
David Plummer (Environment and Climate Change Canada (ECCC), Canada)

NOTE

JN 26565